25. Lapham, L. W. Tetraploid DNA content of Purkinje neurons of human cerebellar cortex. *Science* **159,** 310–312 (1968).
26. Mares, V., Lodin, Z. & Sacha, J. A cytochemical and autoradiographic study of nuclear DNA in mouse Purkinje cells. *Brain Res.* **53,** 273–289 (1973).
27. Doetsch, F., Caille, I., Lim, D. A., Garcia-Verdugo, J. M. & Alvarez-Buylla, A. Subventricular zone astrocytes are neural stem cells in the adult mammalian brain. *Cell* **97,** 703–716 (1999).
28. Spector, D. L., Goldman, R. D. & Leinwand, L. A. *Cells: a Laboratory Manual* 4.1–4.7 (Cold Spring Harbor Laboratory Press, New York, 1998).
29. Hadjantonakis, A. K., Gertsenstein, M., Ikawa, M., Okabe, M. & Nagy, A. Generating green fluorescent mice by germline transmission of green fluorescent ES cells. *Mech. Dev.* **76,** 79–90 (1998).
30. Christensen, J. L. & Weissman, I. L. Flk-2 is a marker in hematopoietic stem cell differentiation: a simple method to isolate long-term stem cells. *Proc. Natl Acad. Sci. USA* **98,** 14541–14546 (2001).

Supplementary Information accompanies the paper on **www.nature.com/nature**.

Acknowledgements The authors thank G. Martin and P. Soriano for transgenic mouse lines, J. Maher at the UCSF Liver Centre for advice and assistance, and M. Kiel, O. Yilmaz and The University of Michigan Flow Cytometry Core for help with flow cytometry. R.P. thanks E. Schaller for technical help. M.A-D. thanks B. Rico, I. Cobos, T. Aragon and U. Borello for personal and scientific support. This work was supported by grants from NIH, the Sandler Foundation, the Spanish Ministry of Science and Technology (Ataxias Cerebelosa), and the Deutsche Forschungsgemeinschaft (DFG). R.P. was the recipient of a postdoctoral fellowship from the Spanish Ministry of Science and Technology.

Competing interests statement The authors declare that they have no competing financial interests.

Correspondence and requests for materials should be addressed to A.A-B. (abuylla@itsa.ucsf.edu).

SNARE-protein-mediated disease resistance at the plant cell wall

Nicholas C. Collins[1]*, Hans Thordal-Christensen[2]*, Volker Lipka[3], Stephan Bau[3], Erich Kombrink[3], Jin-Long Qiu[2], Ralph Hückelhoven[4], Mónica Stein[5], Andreas Freialdenhoven[3], Shauna C. Somerville[5] & Paul Schulze-Lefert[3]

[1]*Sainsbury Laboratory John Innes Centre, Norwich, Norfolk NR4 7UH, UK*
[2]*Plant Research Department, Risø National Laboratory, DK-4000 Roskilde, Denmark*
[3]*Department of Plant Microbe Interactions, Max Planck Institute for Plant Breeding Research, Cologne D-50829, Germany*
[4]*Institute of Phytopathology and Applied Zoology Justus-Liebig-University, Giessen D-35392, Germany*
[5]*Department of Plant Biology, Carnegie Institute of Washington, Stanford, California 94305, USA*

* These authors contributed equally to this work

Failure of pathogenic fungi to breach the plant cell wall constitutes a major component of immunity of non-host plant species—species outside the pathogen host range—and accounts for a proportion of aborted infection attempts on 'susceptible' host plants (basal resistance)[1–4]. Neither form of penetration resistance is understood at the molecular level. We developed a screen for *penetration* (*pen*) mutants of *Arabidopsis*, which are disabled in non-host penetration resistance against barley powdery mildew, *Blumeria graminis* f. sp. *hordei*, and we isolated the *PEN1* gene. We also isolated barley *ROR2* (ref. 2), which is required for basal penetration resistance against *B. g. hordei*. The genes encode functionally homologous syntaxins, demonstrating a mechanistic link between non-host resistance and basal penetration resistance in monocotyledons and dicotyledons. We show that resistance in barley requires a SNAP-25 (synaptosome-associated protein, molecular mass 25 kDa) homologue capable of forming a binary SNAP receptor (SNARE) complex with ROR2. Genetic control of vesicle behaviour at penetration sites, and plasma membrane location of PEN1/ROR2, is consistent with a proposed involvement of SNARE-complex-mediated exocytosis and/or homotypic vesicle fusion events in resistance. Functions associated with SNARE-dependent penetration resistance are dispensable for immunity mediated by race-specific resistance (*R*) genes, highlighting fundamental differences between these two resistance forms.

Most types of plant pathogens fail to produce disease on the majority of plant species. Although 'non-host' resistance is the most common form of resistance, its basis is poorly understood owing to the dearth of tractable genetic systems. This contrasts with 'race-specific' resistance triggered by corresponding *AVIRULENCE (AVR)/R* genes in otherwise compatible host–pathogen interactions, for which many components have been identified[5]. Suicide of cells surrounding the infection site (often referred to as the hypersensitive response) typically accompanies *R*-gene-mediated resistance, and hypersensitive-response-like cell death can also be associated with non-host resistance. These drastic measures form secondary lines of defence that are normally triggered once a fungus has overcome active defences at the plant cell periphery[3,6].

We investigated whether the immunity of the model plant *Arabidopsis* to the barley powdery mildew *B. g. hordei* could be used to develop a system for dissecting non-host resistance. *Blumeria g. hordei* conidiospores germinated on *Arabidopsis* but most sporelings failed to enter the plant cells, accompanied by the formation of a cell wall deposition (papilla) by the plant cell directly beneath penetration attempts. About 10% of sites showed successful penetration as indicated by the presence of a fungal feeding structure (haustorium; Fig. 1a); however, most of the penetrated cells underwent hypersensitive-response-like cell death (Fig. 1b), manifested as whole-cell autofluorescence. Haustoria became encased in deposits containing callose, as revealed by aniline blue staining. Rarely, short hyphae were produced on the leaf surface (Fig. 1a), indicative of successful nutrient uptake through haustoria, before further fungal growth was invariably halted. Independent screens for *Arabidopsis* mutants allowing increased penetration by *B. g. hordei* (*pen* mutants) were performed, using either whole-cell autofluorescence or induced callose deposition as indicators of penetration. Mutants were identified for at least three genes (*PEN1*, *-2* and *-3*; data not shown). Mutant alleles of *PEN1* were recovered from each screen.

Map-based cloning of *PEN1*, supported by the sequencing of four mutant alleles (Fig. 1c), revealed that it encodes *A. thaliana* syntaxin (At)SYP121 (ref. 7). The *pen1-1* mutation results in a stop codon early in the open reading frame and presumably leads to complete loss of PEN1 function. *pen1-1* mutant plants allowed a sevenfold higher incidence of *B. g. hordei* penetration compared with wild-type plants, as well as a concomitant increase in the incidence of hypersensitive-response-like cell death induced by *B. g. hordei* (Fig. 1b). Further *B. g. hordei* growth was invariably arrested in *pen1-1* plants. Thus, although impairment of penetration resistance would be necessary for *Arabidopsis* to be an effective host for *B. g. hordei*, it is not sufficient. *Nicotiana tabacum* SYR1, a tobacco homologue of PEN1/AtSYP121 (AtSYR1), has been suggested to have roles in mediating abscisic acid signalling, stomatal closing and normal growth in tobacco[8]; however, *pen1* mutants showed no discernible defects in general growth, stomatal closing ability, or root development (data not shown).

The barley–*B. g. hordei* combination also provides a useful system for the analysis of penetration resistance. Mutants of the barley *MLO* suppressor of resistance show highly effective penetration resistance against all tested *B. g. hordei* isolates. *ROR1* and *ROR2* were identified in a mutant search as genes required for full *mlo* resistance[2], but they also contribute to low-level basal penetration resistance expressed in 'susceptible' wild-type *MLO* backgrounds (Supplementary Fig. 1a). Combining mutations in *ROR1* and *ROR2* had an additive effect on susceptibility (Supplementary Fig. 1b). We isolated *ROR2* using a barley–rice syntenic-map-based cloning

approach (Supplementary Fig. 2a). A *ROR2* co-segregating syntaxin gene showed a 31-amino-acid in-frame deletion in the mutant *ror2-1* line (ROR2Δ31) (Fig. 1c; see also Supplementary Fig. 2b). Complementation of the *ror2-1* mutation by microprojectile-mediated introduction of a genomic clone driven by the native promoter into leaf epidermal cells confirmed that the gene is *ROR2* (Fig. 1d).

Transgenic *Arabidopsis* plants expressing a green fluorescent protein (GFP)–PEN1 fusion protein from the native *PEN1* promoter revealed a plasma membrane location for PEN1 (Supplementary Fig. 3a). ROR2 also showed a plasma membrane distribution in subcellular fractions analysed using a ROR2 antibody (Supplementary Fig. 3b). Of the 24 syntaxins in *Arabidopsis*[7], PEN1 has the closest resemblance to ROR2 (62% identity and 77% similarity in the cytosolic region; other syntaxins have 55% or less identity and 75% or less similarity; Fig. 1c). A construct containing the *PEN1* coding sequence driven by the barley *ROR2* promoter complemented the penetration phenotype in *ror2-1* mutant plants (Fig. 1d). These data indicate that PEN1 and ROR2 are functionally homologous syntaxin family members possessing a specialized resistance function conserved between monocotyledons and dicotyledons. PEN1 and ROR2 also provide a mechanistic link between non-host and basal penetration resistance.

Syntaxins are members of the SNARE superfamily of proteins that mediate membrane fusion events. SNARE proteins anchored on different membranes interact through their SNARE domains to form a four-helix SNARE bundle, thereby providing much of the energy required to drive membrane fusion[9]. Plasma membrane syntaxins (Qa-SNARE domain) typically combine with a SNAP-25 protein (Qb- and Qc-SNARE domains) and an R-SNARE protein anchored on exocytotic vesicles. Notably, the *pen1-3* substitution alters a glycine that is invariant among all nine *Arabidopsis* subgroup 1 syntaxins, at one of the 16 Qa-SNARE residues that contribute to stabilizing interactions with other SNARE proteins in membrane-fusing complexes[10] (Fig. 1c).

We used a candidate gene approach to identify other factors required for *B. g. hordei* penetration resistance in barley, by silencing homologues of other SNARE proteins or SNARE-associated proteins in leaf epidermal cells. A SNAP-25 homologue was shown to be required for full resistance (construct 1, Fig. 2a), identifying it as a potential binding partner for ROR2 in a resistance-mediating SNARE complex. The product of predicted molecular mass 33.7 kDa was named HvSNAP34 (Supplementary Fig. 4). Owing to the limited silencing often obtained using this system (data not shown), the contribution of HvSNAP34 to resistance may be greater than the 4–7% penetration failure accounted for here. Cells silenced for HvSNAP34 were tested for their ability to mount resistance triggered by the *R* gene *MLA1* (ref. 11), which encodes an intracellular protein containing a nucleotide-binding domain and leucine-rich repeats (Fig. 2b). Resistance against an isolate of *B. g. hordei* containing the corresponding AVRMLA1 determinant was conferred specifically by MLA1 and not by the closely related MLA6, indicating that HvSNAP34 is dispensable for *R*-gene-mediated resistance.

We used the cytosolic regions of wild-type ROR2 and mutant ROR2Δ31 proteins, as well as full-length HvSNAP34, in yeast two-

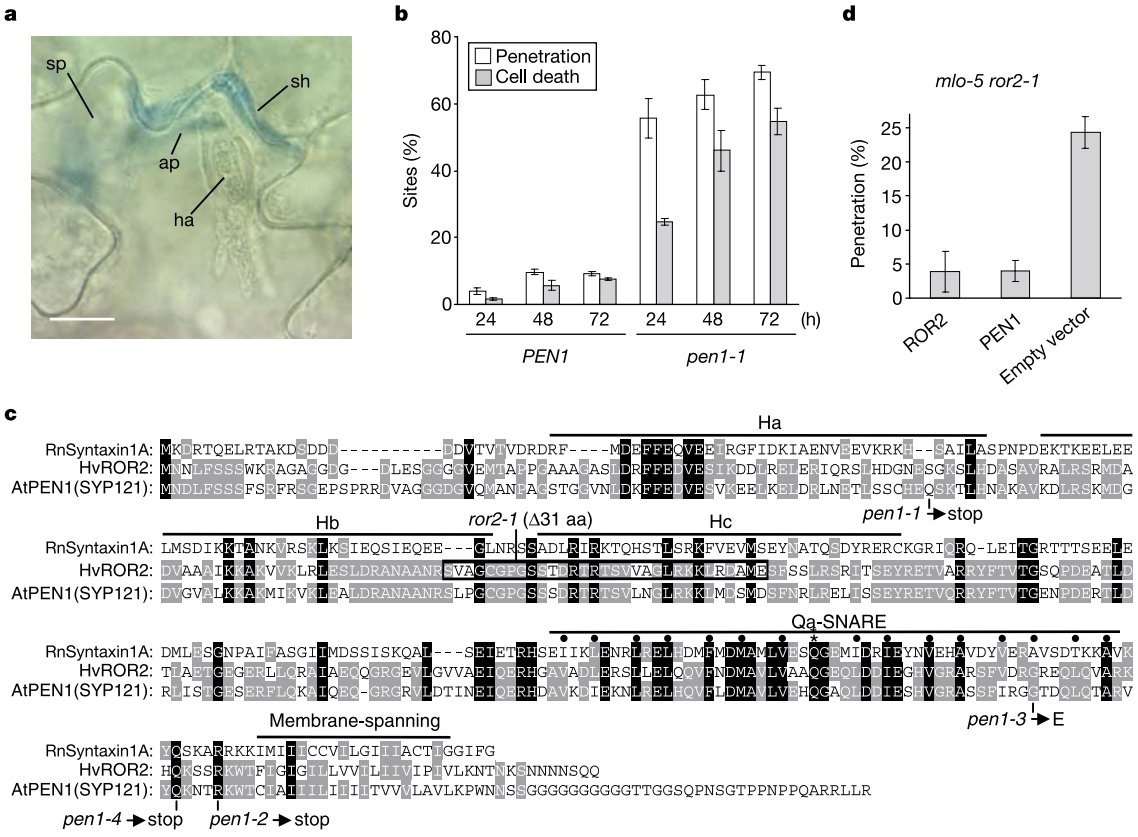

Figure 1 PEN1 and ROR2 are functionally homologous syntaxins. **a**, Multidigitate haustorium (ha) formed by *B. g. hordei* in a wild-type *PEN1 Arabidopsis* epidermal cell after successful cell wall penetration. External fungal structures are stained blue. ap, appressorium; sh, secondary hypha; sp, conidiospore. Scale bar, 10 μm. **b**, Frequency of penetration and cell death at *B. g. hordei–Arabidopsis* interaction sites. The times indicated are times after inoculation. **c**, ROR2 and PEN1 mutations. Rat neuronal syntaxin 1A is included to show positions in the Qa-type SNARE domain that contribute to stabilizing ionic (asterisk) or hydrophobic (black circle) interactions with other SNARE proteins[10,24], and to show locations of Ha, Hb and Hc helices[12]. **d**, Complementation of the *ror2-1* mutation in barley by *ROR2* and *PEN1*. Expression constructs were introduced into leaf epidermal cells of the *mlo-5 ror2-1* partially susceptible genotype.

hybrid protein interaction assays (Fig. 3a). Both forms of ROR2 interacted with HvSNAP34; however, the Δ31 deletion strongly enhanced binding to HvSNAP34 in addition to allowing formation of ROR2Δ31 homomultimers (Fig. 3a). In other plasma membrane syntaxins, the amino terminus forms an autonomously folded bundle comprising helices Ha, Hb and Hc (Fig. 1c), which binds reversibly with the Qa-SNARE domain, suppressing interactions with other SNARE proteins and the formation of high-order homomultimers *in vitro*[12–14]. The Δ31 deletion covers most of the predicted Hc helix (Fig. 1c). Therefore, the altered SNARE binding of ROR2Δ31 is probably due to disruption of similar intramolecular interactions within ROR2, leading to a constitutively open state.

The ROR2Δ31 protein produced by the endogenous *ror2-1* allele is unaltered in membrane location, and is only slightly reduced in abundance (Supplementary Fig. 3b), suggesting that its inability to confer resistance is due to disruption of a critical biochemical function requiring the region deleted in this protein. Notably, overexpressed ROR2Δ31 acted as a potent inhibitor of resistance in a wild-type ROR2 background (Fig. 3b), probably by sequestering interacting partner(s) of ROR2 (for example, HvSNAP34) into non-functional complexes. Overexpression of ROR2Δ31 also increased susceptibility in a mutant *ror2-1* background (Fig. 3c), suggesting that either the *ror2-1* mutant retains partial ROR2 activity, or that another syntaxin sharing interacting partner(s) with ROR2 contributes to the resistance. Cells overexpressing ROR2Δ31 were able to mount resistance triggered by the *R* gene *MLA1* (Fig. 3d), reinforcing the notion that SNARE functions related to penetration resistance are not critical for *R*-gene-mediated resistance.

Because the requirement for SNARE proteins implies a role for membrane fusion in resistance, we examined whether the incidence of *B. g. hordei*-associated vesicles detectable by light microscopy (>1 μm) was altered by mutations in the *MLO*, *ROR1* and *ROR2* genes. Consistent with previous observations[15], large (2–3 μm) vesicles containing H_2O_2 could be observed in the host cells beneath appressoria (Fig. 4a). Vesicles appeared to aggregate and coalesce with time, and disappeared by 72 h at sites of primary penetration attempts (not shown). The appearance of vesicles was significantly influenced by mutations in each of the *MLO*, *ROR1* and *ROR2* genes, with vesicle incidence being positively associated with levels of resistance to *B. g. hordei* penetration (Fig. 4b).

Our findings obtained here (Figs 1b, 2b and 3d) and previously[6] show that components of penetration resistance, including SNARE-related functions, are not critical for *R*-gene-mediated, race-specific resistance or for secondary lines of non-host resistance. Moreover, *PEN1*, *-2* and *-3* differ from genes uncovered by searches for

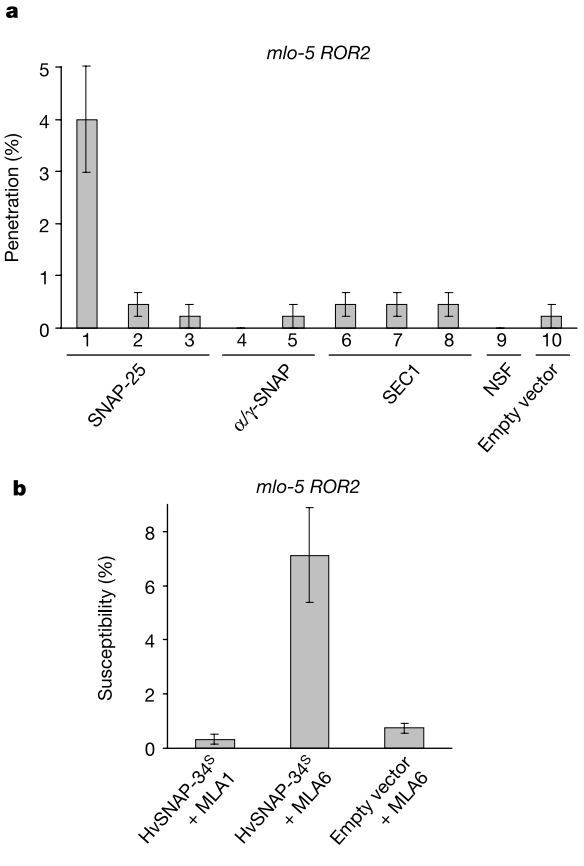

Figure 2 The barley SNAP-25 homologue HvSNAP34 is required for penetration resistance. **a**, Barley homologues of SNARE and SNARE-associated proteins were silenced in the highly resistant *mlo-5 ROR2* genotype. Representative mammalian homologues are used to indicate protein classes. Construct 1 targets HvSNAP34. GenBank accession numbers of targeted genes are listed in Methods. **b**, HvSNAP34-silenced cells retain MLA1-mediated race-specific resistance. The HvSNAP34 silencing (superscript s) construct was co-introduced with MLA1 or MLA6 *R*-gene constructs before challenge with the *B. g. hordei* isolate K1, which is recognized by MLA1 but not MLA6. Susceptibility of HvSNAP34^S plus MLA6 cells provided a control for both impairment of penetration resistance and *R*-gene-mediated resistance specificity.

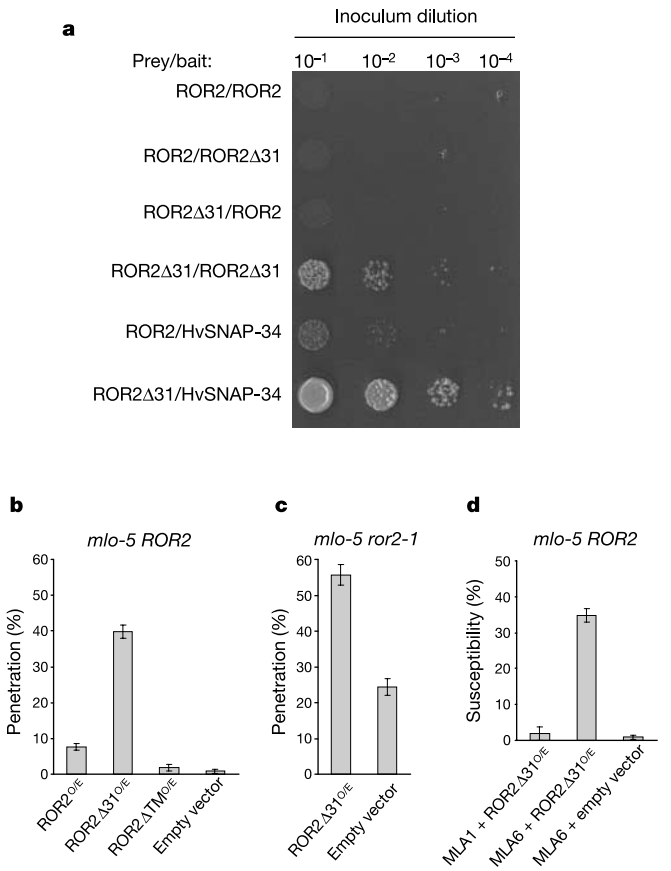

Figure 3 ROR2 interactions and overexpression. **a**, Yeast two-hybrid protein–protein interaction assays. Yeast cells were spotted on to a medium lacking histidine, upon which subsequent growth depends on interaction between bait and prey. **b**, **c**, Overexpression (O/E) constructs were introduced into barley leaves of the genotypes indicated. **d**, Cells overexpressing ROR2Δ31 retain MLA1-mediated race-specific resistance. The overexpression construct was co-introduced with MLA1 or MLA6 *R*-gene constructs before challenge with a *B. g. hordei* strain that is recognized by MLA1 but not MLA6. Susceptibility of ROR2Δ31$^{O/E}$ plus MLA6 cells provided a control for both impairment of penetration resistance and *R*-gene-mediated resistance specificity.

enhanced disease susceptibility mutants performed in contexts of high penetration incidence in compatible host–pathogen interactions (ref. 5 and our own unpublished data). Thus, basal/non-host resistance processes responsible for halting early stages of fungal ingress seem to act independently of other resistance types.

Three lines of evidence suggest that PEN1 and ROR2 mediate resistance by participating in SNARE complexes. First, resistance also requires the Qa- and Qb-SNARE-containing protein HvSNAP34. Second, the *pen1-3* substitution alters one of the Qa-SNARE positions that contribute to stabilizing interactions with other SNARE proteins. Third, the potent resistance inhibition observed upon ROR2Δ31 overexpression, together with the enhanced binding of ROR2Δ31 to HvSNAP34, is consistent with deregulated formation of binary SNARE complexes, which normally serve as transient intermediates in assembly of ternary complexes containing the additional R-SNARE.

The plasma membrane location of PEN1 and ROR2 may facilitate exocytosis; however, the reduced incidence of *B. g. hordei*-induced vesicles in the *ror2-1* mutant defies this simple interpretation. One possibility is that, in addition to facilitating exocytosis, ROR2 may also mediate homotypic fusion of vesicles to one another, in a manner similar to KNOLLE syntaxin-dependent homotypic vesicle fusion at the growing cell plate[16]. Homotypic fusion could allow the vesicles to achieve a size visible by light microscopy, and might account for the fact that the vesicles are relatively large compared with most exocytotic vesicles described in animals and plants[17,18]. One constituent of the vesicles is H_2O_2, a plant defence compound that can perform antimicrobial, cell-wall crosslinking and signalling functions[19]. Interestingly, the *B. g. hordei*-induced vesicles resemble, both in size and behaviour, coloured antimicrobial-compound-containing vesicles that coalesce in sorghum leaf epidermal cells beneath sites of attempted penetration by the fungus *Colletotrichum graminicola*[20]. Vesicles destined for exocytosis contain R-SNAREs, which join with binary syntaxin–SNAP-25 complexes on the plasma membrane to drive membrane fusion[9]. If vesicle-anchored R-SNARE partners of ROR2 and PEN1 can be identified they may allow isolation of vesicles critical for resistance, and their cargo. □

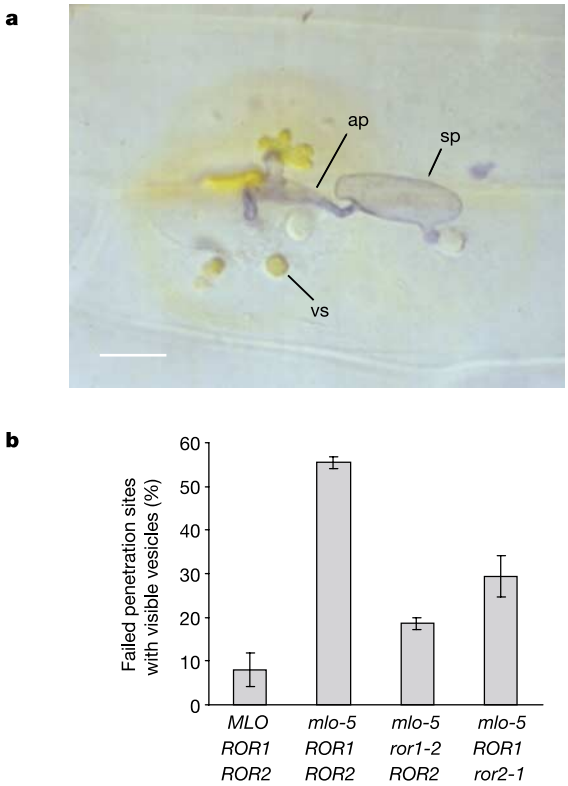

Figure 4 *Blumeria graminis hordei*-induced vesicles. **a**, A failed *B. g. hordei* penetration attempt with vesicles in barley cells. Fungal structures are stained blue. A vesicle (vs) is indicated. Brown DAB staining indicates the presence of H_2O_2. Scale bar: 10 μm. **b**, The incidence of *B. g. hordei*-induced vesicles is under genetic control. Interaction sites were classified as positive or negative for the presence of vesicles visible at ×400 magnification (approximately 1.0 μm or greater).

Methods

Arabidopsis pen1 mutant screen

M_2 populations were derived by ethylmethane sulphonate treatment of *Arabidopsis* Columbia (Col-0 or Col-3 *gl1*). In the two screens yielding *pen-1*, *-2* and *-4*, M_2 plants were inoculated with *B. g. hordei* isolate CR3, and after 48 h detached leaves were subjected to aniline blue epifluorescence staining to monitor callose[21] deposited in response to penetration. In the screen yielding *pen1-3*, M_2 plants were inoculated with *B. g. hordei* isolate K1, and 72 h later examined with ultraviolet light (excitation filter 365/12 nm; dichroic mirror 400LP) to monitor the autofluorescence resulting from the hypersensitive-response-like cell death triggered by penetration. The *pen* mutants were deposited in the *Arabidopsis* Stock Centre.

Quantification of *pen1-1* mutant phenotype

Individual *Arabidopsis*–*B. g. hordei* interaction sites were characterized for penetration success using aniline blue and for the hypersensitive-response-like cell death using ultraviolet autofluorescence. Three repetitions, scoring 100 sites per time point and genotype, were performed.

PEN1 cloning

PEN1 was mapped using a Columbia *pen1-1* × Landsberg *erecta* F_2 population of 474 individuals using standard polymerase chain reaction (PCR)-based marker techniques.

ROR2 syntenic mapping and *ROR2* sequencing

See Supplementary Information. Full-length *ROR2* messenger RNA (AY246907) and genomic (AY246906) sequences were derived by rapid amplification of cloned ends and adaptor-mediated PCR methods.

Barley expression and silencing constructs

The BAC clone HvMBa693F23 was identified from the genomic DNA library of wild-type *ROR2* barley cv. Morex[22] by screening with a *ROR2* probe. Complementation with *ROR2* was performed using a HvMBa693F23 subclone containing the *ROR2* open reading frame flanked by 881 base pairs (bp) of 5′ sequence and 81 bp of 3′ sequence. The *PEN1* complementation construct contained the *PEN1* genomic coding sequence and terminator inserted behind 3.4 kilobases of *ROR2* 5′ untranslated region sequence. The fusion junction followed the ATG, resulting in a D to N substitution at the third position of the encoded PEN1 protein, which is otherwise identical to PEN1.

Overexpression constructs were made using the pUBI-Adaptor-NOS vector[11] containing the strong constitutive maize polyubiquitin (UBI) promoter. The ROR2ΔTM construct encoding the ROR2 cytosolic region was made by introducing a T285stop mutation. We confirmed PCR-derived clones by sequencing.

Homologues of SNARE or SNARE-associated proteins were identified in tBLASTn searches of the Syngenta TMRI rice genomic sequence database (http://portal.tmri.org/rice/RiceDescription.html) and the Triticeae expressed sequence tag and rice genomic sequence databases (NR and HTGS) at NCBI. Silencing fragments for HvSNAP34 spanned nucleotide positions 639–982 (coding) or 1007–1275 (3′ untranslated region) of the complementary DNA (AY247208). Other genes (GenBank accession numbers AY247209 to AY247214, AJ466709 and AV833528) were targeted for silencing using fragments of 115–351 bp. The pUAMBN silencing vector contains the UBI promoter and *MLA1* intron 3 located between two *att*L1–*ccd*B–*att*L2 cassettes for cloning inserts in inverted orientation using Gateway technology (Life Technologies).

R gene and GUS reporter constructs have been described[11].

Single-cell gene expression and silencing

Gene expression and silencing in barley leaf epidermal cells was performed essentially as described[11]. Gold microprojectiles (1.0 μm) were coated with a total of 12 μg plasmid DNA mixture per shot, using 8 μg of double-stranded RNAi construct, 0.6 μg of complementation construct but otherwise equal amounts of other constructs. Bombarded leaves were inoculated with *B. g. hordei* isolate K1 after 96 h (silencing) or 4 h (expression), and penetration frequencies were determined 48 h after inoculation. Generally, 150 interaction sites were assessed from each of three to four independent 'shootings' per construct combination. *MLA1* and *MLA6 R* genes confer pre-haustorial resistance in this system due to an overexpression effect[11]. Hence, in tests involving both penetration resistance and *R*-gene-mediated resistance, susceptibility was scored on the basis of haustorium formation.

Yeast two-hybrid analysis

Yeast two-hybrid tests were performed using the GAL4 system with the *HIS* reporter in yeast strain AH109 essentially as recommended by the suppliers (Clontech). Vectors (supplied by J. Uhrig) were made by adapting pACT2 and pAS2-1 (Clontech) to accept inserts using Gateway cloning technology (Life Technologies). PCR-derived cDNA clones were verified by sequencing, and the prey and bait constructs were co-transformed into

yeast. Liquid culture densities were equalized using absorption at 600 nm, and 10 µl of each dilution was spotted on to histidine minus medium before incubation.

Vesicle analysis

Vesicle analysis was performed on leaf segments stained with DAB to detect H_2O_2 as described[15]. Leaves of 7-day-old seedlings were inoculated with *B. g. hordei*, and 24 h later they were assessed by differential interference contrast microscopy for vesicles in the short cells of the adaxial epidermis[23]. Per genotype, 100 sites were scored from each of three leaves. Only sites at which penetration had failed were scored.

See Supplementary Information for barley genotype analysis with *B. g. hordei*, and PEN1 and ROR2 localization.

Received 16 June; accepted 15 September 2003; doi:10.1038/nature02076.

1. Johnson, L. E. B., Bushnell, W. R. & Zeyen, R. J. Defense patterns in nonhost higher plant species against two powdery mildew fungi. I. Monocotyledonous species. *Can. J. Bot.* **60,** 1068–1083 (1982).
2. Freialdenhoven, A., Peterhänsel, C., Kurth, J., Kreuzaler, F. & Schulze-Lefert, P. Identification of genes required for the function of non-race-specific *mlo* resistance to powdery mildew in barley. *Plant Cell* **8,** 5–14 (1996).
3. Hoogkamp, T. J. H., Chen, W. Q. & Niks, R. E. Specificity of prehaustorial resistance to *Puccinia hordei* and to two inappropriate rust fungi in barley. *Phytopathology* **88,** 856–861 (1998).
4. Mellersh, D. G., Foulds, I. V., Higgins, V. J. & Heath, M. C. H_2O_2 plays different roles in determining penetration failure in three diverse plant-fungal interactions. *Plant J.* **29,** 257–268 (2002).
5. Hammond-Kosack, K. E. & Parker, J. E. Deciphering plant-pathogen communication: fresh perspecitives for molecular resistance breeding. *Curr. Opin. Biotechnol.* **14,** 177–193 (2003).
6. Peterhänsel, C., Freialdenhoven, A., Kurth, J., Kolsch, R. & Schulze-Lefert, P. Interaction analyses of genes required for resistance responses to powdery mildew in barley reveal distinct pathways leading to leaf cell death. *Plant Cell* **9,** 1397–1409 (1997).
7. Sanderfoot, A. A., Assaad, F. F. & Raikhel, N. V. The *Arabidopsis* genome. An abundance of soluble *N*-ethylmaleimide-sensitive factor adaptor protein receptors. *Plant Physiol.* **124,** 1558–1569 (2000).
8. Blatt, M. R. Toward understanding vesicle traffic and the guard cell model. *New Phytol.* **153,** 405–413 (2002).
9. Jahn, R., Lang, T. & Südhof, T. C. Membrane fusion. *Cell* **112,** 519–533 (2003).
10. Fasshauer, D., Sutton, R. B., Brunger, A. T. & Jahn, R. Conserved structural features of the synaptic fusion complex: SNARE proteins reclassified as Q- and R-SNAREs. *Proc. Natl Acad. Sci. USA* **95,** 15781–15786 (1998).
11. Shen, Q. H. *et al.* Recognition specificity and RAR1/SGT1 dependence in barley *Mla* disease resistance genes to the powdery mildew fungus. *Plant Cell* **15,** 732–744 (2003).
12. Lerman, J. C., Robblee, J., Fairman, R. & Hughson, F. M. Structural analsysis of the neuronal SNARE protein syntaxin-1A. *Biochemistry* **39,** 8470–8479 (2000).
13. Munson, M., Chen, X., Cocina, A. E., Schultz, S. M. & Hughson, F. M. Interactions within the yeast t-SNARE Sso1p that control SNARE complex assembly. *Nature Struct. Biol.* **7,** 894–902 (2000).
14. Misura, K. M. S., Scheller, R. H. & Weis, W. I. Self-association of the H3 region of syntaxin 1A. *J. Biol. Chem.* **276,** 13273–13282 (2001).
15. Hückelhoven, R., Fodor, J., Preis, C. & Kogel, K. H. Hypersensitive cell death and papilla formation in barley attacked by the powdery mildew fungus are associated with hydrogen peroxide but not with salicylic acid accumulation. *Plant Physiol.* **119,** 1251–1260 (1999).
16. Lauber, M. H. *et al.* The *Arabidopsis* KNOLLE protein is a cytokinesis-specific syntaxin. *J. Cell Biol.* **139,** 1485–1493 (1997).
17. Betz, W. J. & Richards, D. A. What goes out must come in. *Nature Neurosci.* **3,** 636–637 (2000).
18. Emans, N., Zimmerman, S. & Fischer, R. Uptake of fluorescent marker in plant cells is sensitive to brefeldin A and wortmannin. *Plant Cell* **14,** 71–86 (2002).
19. Lamb, C. & Dixon, R. A. The oxidative burst in plant disease resistance. *Annu. Rev. Plant Physiol. Plant Mol. Biol.* **48,** 251–275 (1997).
20. Snyder, B. A. & Nicholson, R. L. Synthesis of phytoalexins in sorghum as a site-specific response to fungal ingress. *Science* **248,** 1637–1639 (1990).
21. Adam, L. & Somerville, S. C. Genetic characterization of five powdery mildew disease resistance loci in *Arabidopsis thaliana*. *Plant J.* **9,** 341–356 (1996).
22. Yu, Y. *et al.* A bacterial artificial chromosome library for barley (*Hordeum vulgare* L.) and the identification of clones containing putative resistance genes. *Theor. Appl. Genet.* **101,** 1093–1099 (2000).
23. Koga, H., Bushnell, W. R. & Zeyen, R. J. Specificity of cell type and timing of events associated with papilla formation and the hypersensitive reaction in leaves of *Hordeum vulgare* attacked by *Erysiphe graminis* f. sp *hordei*. *Can. J. Bot.* **68,** 2344–2352 (1990).
24. Sutton, R. B., Fasshauer, D., Jahn, R. & Brunger, A. T. Crystal structure of a SNARE complex involved in syntaptic exocytosis at 2.4 Å resolution. *Nature* **395,** 347–353 (1998).

Supplementary Information accompanies the paper on **www.nature.com/nature**.

Acknowledgements This work was supported by Syngenta, the Max Planck Society, the Gatsby Charitable Foundation, the Danish Agricultural and Veterinary Research Council, the GABI Non-host Resistance Consortium (Bundesministerium für Bildung und Forschung), the Carnegie Institution of Washington, and the US Department of Energy. M.S. was supported in part by a Stanford Graduate Fellowship. N.C.C. thanks the host group of K. Shirasu in the Sainsbury Laboratory. We thank R. Bradbourne and H. Tippmann for technical assistance; M. Gale for microsatellite primers; M. Miklis and J. Uhrig for silencing and yeast two-hybrid vectors; R. Serrano and R. Napier for H^+-ATPase and CALRETICULIN antisera; and R. Oliver for the GUS reporter construct.

Competing interests statement The authors declare that they have no competing financial interests.

Correspondence and requests for materials should be addressed to P.S.-L. (schlef@mpiz-koeln.mpg.de). Sequences are deposited in GenBank under accession numbers AY246893 to AY246907 and AY247208 to AY247214.

Bone recognition mechanism of porcine osteocalcin from crystal structure

Quyen Q. Hoang[1,2], Frank Sicheri[3,4], Andrew J. Howard[5] & Daniel S. C. Yang[1]

[1]*Department of Biochemistry, Faculty of Health Science, McMaster University, Hamilton, Ontario L8N 3Z5, Canada*
[2]*Microstar Biotech Inc., 7 Innovation Drive, Flamborough, Ontario L9H 7H9, Canada*
[3]*Program in Molecular Biology and Cancer, Samuel Lunenfeld Research Institute, Mount Sinai Hospital, 600 University Avenue, Toronto, Ontario M5G 1X5, Canada*
[4]*Department of Molecular and Medical Genetics, University of Toronto, Toronto, Ontario M5S 1A8, Canada*
[5]*Department of Biological, Chemical and Physical Sciences, Illinois Institute Technology, Chicago, Illinois 60616, USA*

Osteocalcin is the most abundant noncollagenous protein in bone[1], and its concentration in serum is closely linked to bone metabolism and serves as a biological marker for the clinical assessment of bone disease[2]. Although its precise mechanism of action is unclear, osteocalcin influences bone mineralization[3,4], in part through its ability to bind with high affinity to the mineral component of bone, hydroxyapatite[5]. In addition to binding to hydroxyapatite, osteocalcin functions in cell signalling and the recruitment of osteoclasts[6] and osteoblasts[7], which have active roles in bone resorption and deposition, respectively. Here we present the X-ray crystal structure of porcine osteocalcin at 2.0 Å resolution, which reveals a negatively charged protein surface that coordinates five calcium ions in a spatial orientation that is complementary to calcium ions in a hydroxyapatite crystal lattice. On the basis of our findings, we propose a model of osteocalcin binding to hydroxyapatite and draw parallels with other proteins that engage crystal lattices.

The primary structure of osteocalcin (OC) is highly conserved among vertebrates and contains three vitamin-K-dependent γ-carboxylated glutamic acid (Gla) residues at positions 17, 21 and 24 in porcine OC (pOC; Fig. 1a and Supplementary Fig. 1). Solution studies have shown that mature OC is largely unstructured in the absence of calcium and undergoes a transition to a folded state on the addition of physiological concentrations of calcium[8]. NMR analysis has shown that OC is a globular protein consisting of α-helical secondary structure in its folded state[8,9], but the detailed three-dimensional structure of OC has not been forthcoming.

To gain further insight into the structure of OC and its ability to recognize the hydroxyapatite (HA) mineral component of bone, we have determined the crystal structure of pOC at 2.0 Å using the Iterative Single Anomalous Scattering method[10]. Bijvoet difference Patterson map analysis detected the presence of three tightly bound Ca^{2+} ions and two S atoms corresponding to a disulphide bridge between Cys 23 and Cys 29, which together were used to phase the pOC structure. An atomic model corresponding to residues Pro 13 to Ala 49 was built into well-defined electron density (Supplementary Fig. 2) and refined to an R_{work} and R_{free} of 25.5% and 28.3%, respectively. Data collection and structure refinement statistics are summarized in Supplementary Table 1.

pOC forms a tight globular structure comprising a previously unknown fold (no matches in the DALI database[11]) with a topology consisting, from its amino terminus, of three α-helices (denoted α1–α3) and a short extended strand (denoted Ex1; Fig. 1b). Helix α1 and helix α2 are connected by a type III turn structure from Asn 26 to Cys 29 and form a V-shaped arrangement that is stabilized